IMPEDANCE MEASUREMENTS OF NONUNIFORM TRANSMISSION LINES IN TIME DOMAIN USING AN IMPROVED RECURSIVE MULTIPLE REFLECTION COMPUTATION METHOD

Y. Liu [*], L. Tong, W.-X. Zhu, Y. Tian, and B. Gao

School of Automation Engineering, University of Electronic Science and Technology of China, Chengdu, Sichuan 611731, China

Abstract—In this paper, a recursive computation method is developed to derive the multiple reflections of nonuniform transmission lines. The true impedance profiles of the nonuniform transmission lines are then reconstructed with the help of this method. This method is more efficient than other algorithm. To validate this method, two nonuniform microstrip lines are designed and measured using Agilent vector network analyzer E8363B from 10 MHz to 20 GHz with 10 MHz interval. The reflection coefficients of these nonuniform microstrip lines in time domain are attained from the scattering parameters using inverse Chirp-Z transform. The reconstructed characteristic impedance profiles of the nonuniform lines are compared with those reconstructed by Izydorczyk's algorithm. The agreements of the results illustrate the validity of the recursive multiple reflection computation method in this paper.

1. INTRODUCTION

Planar microwave transmission lines such as microstrip lines and coplanar waveguides are widely used in microwave circuits and high-speed digital circuits, for example, antenna [1], power dividers [2] and filters [3]. The performances of microwave circuits and high-speed digital circuits in time domain are much concerned by designers [4–10]. As a basic measurement technique in time domain, the Time Domain Reflectometry (TDR) is widely used to acquire the transient response of the circuits [8, 9] in time domain. And as a basic measurement instrument in frequency domain, Vector Network Analyzer (VNA),

with the help of inverse Fourier transform algorithm, is also able to obtain the time-domain response the same as TDR if sufficient bandwidth is provided [11, 12]. Therefore, the time domain responses of microwave circuits and high-speed digital circuits can be attained by both TDR and VNA. And the impedance profiles of the circuits then can be calculated according to their time-domain responses. However, multiple reflections of a nonuniform transmission line always result in incorrect impedance readouts [13, 14]. The true impedance profiles need to be reconstructed from the confusing measurement results.

Many authors have made significant contributions to the study of reconstructing the true impedance profiles of nonuniform transmission lines from the data acquired by TDR or VNA [13–19]. The literature [15] used a recursive method with only three variables Γ_{table}, Γ_{open} and $\Gamma_{matched}$. However, the processing time of this algorithm is in the order of $o(N^3)$, that is if the number of data doubles, the computation time will be roughly eight times longer. The literature [16] used the extended peeling algorithm to extract the circuit model of lossy interconnects from the TDR/T measurement data. However, to implement this algorithm, the resistance per unit length of the circuits must be measured by TDR firstly. Hsue and Pan [13] divided the reflected wave into many time durations with equal length and decomposed the reflected wave into 'wavefront' and 'nonwavefront' components, which make it intuitional to reconstruct the nonuniform transmission lines. However, the expression of the reflected wave $V_r(t)$ in [13] and [19] is complicated and difficult to realize. Izydorczyk [20, 21] proposed an algorithm to reconstruct the impedances of nonuniform transmission lines, which is simple and easy to use. The Izydorczyk's algorithm used the relationship between the voltages at the nth layer and the $(n + 1)$th layer and the algorithm is in the order of $o(N^2)$.

In this paper, a lattice diagram [14, 15] that is used to illustrate the process of the injected step voltage generated by TDR propagating in a nonuniform transmission line is studied. Then a recursive algorithm is developed to calculate the reflected wave $V_r(t)$. This algorithm calculates the voltages injected into the lattices recursively from the unit step response of the nonuniform transmission line. The response is acquired by TDR or VNA and includes multiple reflections. The true impedance profile of the transmission line can be reconstructed with the help of this algorithm. To validate the algorithm, two nonuniform microstrip lines are designed and measured using Agilent VNA E8363B from 10 MHz to 20 GHz with 10 MHz interval. The unit step responses are attained from S_{11} of the circuits using inverse Chirp-Z transform (ICZT). The reconstructed

characteristic impedance profiles of the nonuniform lines are compared with those reconstructed by Izydorczyk's algorithm. The agreements of the reconstructed results illustrate the validity of the recursive multiple reflection computation method in this paper.

2. THEORY

2.1. An Improved Recursive Method for Multiple Reflection Computation

The first step of analyzing a nonuniform transmission line is to divide it. Suppose a nonuniform transmission line can be decomposed into a series of uniform transmission line segments. This assumption is reasonable if the number of segments is large enough. And suppose the time that it takes for the voltage traveling through each segment are the same. The lattice diagram that illustrates the injected voltage traveling back and forth in the nonuniform transmission line is shown in Figure 1. In Figure 1 the nonuniform transmission line is decomposed into n uniform transmission line segments, each of which holds a impedance of Z_i, $(i = 1, 2, \ldots, n)$. Z_0 is the characteristic impedance of measurement instruments. As to TDR and VNA, Z_0 is the characteristic impedance of the test ports. Therefore, there is a discontinuity between adjacent uniform segments. For two adjacent segments, sometimes, the impedances of which are equal to each other, but we still think there is a discontinuity which can not cause any reflections. Therefore, there are n discontinuities along the nonuniform
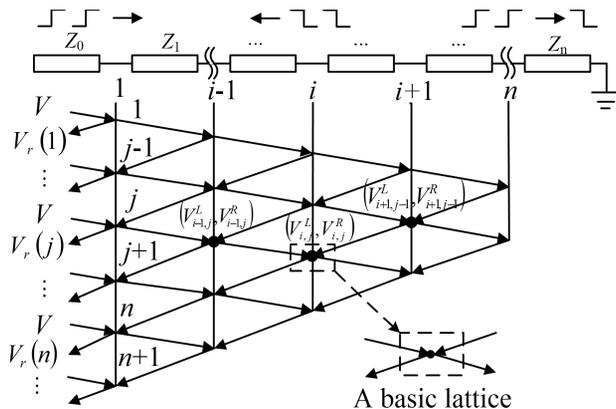

Figure 1. A lattice diagram that illustrates the injected voltage traveling back and forth in a nonuniform transmission line.

transmission line. The TDR samples the reflected voltage at equal time intervals, say Δt. Let the time that it takes for the voltage traveling through each uniform segment be τ, therefore, Δt is equal to 2τ. In the procedure of construction, which is illustrated in Section 2.2, the reflect voltages are sampled by TDR with equal time interval. If the reflect voltages at the test port are known, the lattice diagram in Figure 1 are established. Therefore, the nonuniform transmission lines are not divided actually.

A basic lattice that is also called a cell [16] is defined in Figure 1. Let i denote the ith discontinuity and j denote the jth time interval, in other words, the time of $j\Delta t$. All lattices in Figure 1 are indexed with i and j. The voltage injected into the lattice (i, j) can be denoted as $(V_{i,j}^L, V_{i,j}^R)$, where $V_{i,j}^L$ denotes the voltage that injected into the lattice (i, j) from its left lattice and $V_{i,j}^R$ denotes the voltage that injected into the lattice (i, j) from its right lattice. It is clear in Figure 1 that the left lattice and the right lattice of lattice (i, j) are lattice $(i - 1, j)$ and lattice $(i + 1, j - 1)$ respectively. As shown in Figure 1, part of $V_{i,j}^L$ is reflected back to the left side by the ith discontinuity and the rest passes through. Just as $V_{i,j}^L$, part of $V_{i,j}^R$ is reflected back to the right side and the rest passes through and travels to the test port.

Therefore, the relationship of the lattices can be determined. For $2 \leq i < n$ and $j \geq 2$, the voltage $V_{i,j}^L$ that is injected into the lattice (i, j) contains two parts: the first part is portion of $V_{i-1,j}^L$ that travels through lattice $(i - 1, j)$ and the other is portion of $V_{i-1,j}^R$ that is reflected back by the $(i - 1)$th discontinuity. Therefore, $V_{i,j}^L$ can be expressed by (1a). $V_{i,j}^R$ can be derived in the same way, just shown in (1b).

$$V_{i,j}^L = T_{i-2,i-1}V_{i-1,j}^L + \Gamma_{i-1,i-2}V_{i-1,j}^R \tag{1a}$$

$$V_{i,j}^R = \Gamma_{i,i+1}V_{i+1,j-1}^L + T_{i+1,i}V_{i+1,j-1}^R \tag{1b}$$

where $T_{i,i+1}$ and $T_{i+1,i}$ are the transmission coefficients; $\Gamma_{i,i+1}$ and $\Gamma_{i+1,i}$ are the reflection coefficients between Z_i and Z_{i+1}. $\Gamma_{i,i+1}$, $\Gamma_{i+1,i}$, $T_{i,i+1}$ and $T_{i+1,i}$ are defined as follows.

$$\Gamma_{i,i+1} = \frac{Z_{i+1} - Z_i}{Z_{i+1} + Z_i} = -\Gamma_{i+1,i} \tag{2a}$$

$$T_{i,i+1} = 1 + \Gamma_{i,i+1} \tag{2b}$$

$$T_{i+1,i} = 1 + \Gamma_{i+1,i} \tag{2c}$$

For the lattices such that $i = 1$ and $j \geq 2$, the voltage injected into the lattices from left side is generated by TDR and remains constant,

therefore

$$V_{i,j}^L = V \qquad (3a)$$

$$V_{i,j}^R = \Gamma_{i,i+1}V_{i+1,j-1}^L + T_{i+1,i}V_{i+1,j-1}^R \qquad (3b)$$

where the value of V in (3a) and (6a) which is shown later is the magnitude of the step voltage generated by TDR. To normalize the reflected voltage, the value of V is assigned to be $1\,\mathrm{V}$.

For the lattices such that $2 \leq i < n$ and $j = 1$, there are no voltages injecting into their left lattices indexed with $i - 1$ and j from the right sides and there are no right lattices indexed with $i + 1$ and $j - 1$. Therefore, (1a) and (1b) are rewritten as follows.

$$V_{i,j}^L = T_{i-2,i-1}V_{i-1,j}^L \qquad (4a)$$

$$V_{i,j}^R = 0 \qquad (4b)$$

For the lattices such that $i = n$ and $j \geq 2$, there are no right lattices which are indexed with $i + 1$ and $i - 1$. Therefore, $V_{i,j}^L$ and $V_{i,j}^R$ are represented as follows.

$$V_{i,j}^L = T_{i-2,i-1}V_{i-1,j}^L + \Gamma_{i-1,i-2}V_{i-1,j}^R \qquad (5a)$$

$$V_{i,j}^R = 0 \qquad (5b)$$

For the lattice such that $i = 1$ and $j = 1$,

$$V_{i,j}^L = V \qquad (6a)$$

$$V_{i,j}^R = 0 \qquad (6b)$$

And for $i > n$ and $j \geq 1$, the lattices indexed with i and j are viewed as 'virtual' lattices and $V_{i,j}^L$ and $V_{i,j}^R$ are assigned to be zero, which may be useful for programming.

The analysis above can be summarized by the equations as follows.

$$V_{i,j}^L = \begin{cases} T_{i-2,i-1}V_{i-1,j}^L, & 2 \leq i \leq n, \ j = 1 \\ T_{i-2,i-1}V_{i-1,j}^L + \Gamma_{i-1,i-2}V_{i-1,j}^R, & 2 \leq i \leq n, \ j \geq 2 \\ 1, & i = 1, \ j \geq 1 \\ 0, & \text{otherwise} \end{cases} \qquad (7)$$

$$V_{i,j}^R = \begin{cases} \Gamma_{i,i+1}V_{i+1,j-1}^L + T_{i+1,i}V_{i+1,j-1}^R, & 1 \leq i < n, \ j \geq 2 \\ 0, & \text{otherwise} \end{cases} \qquad (8)$$

The reflected voltage measured by TDR at the time of $j\Delta t$ can be expressed by

$$V_r(j) = T_{1,0}V_{1,j}^R + \Gamma_{0,1}V_{1,j}^L \qquad (9)$$

where $j = 1, 2, 3, \ldots$.

The process of multiple reflection computation is to calculate the reflect voltages at the test port according to the impedances of the uniform line segments. But by contrast, the process of impedance reconstruction is to obtain the impedance of the uniform line sections under the condition that V_r is measured by TDR or VNA.

2.2. Impedance Reconstruction

For $i = 1$, the reflected coefficient $\Gamma_{0,1}$ and impedance Z_1 can be obtained directly from the measured data.

$$\Gamma_{0,1} = V_r(1) \tag{10}$$

$$Z_1 = Z_0 \frac{1 + \Gamma_{0,1}}{1 - \Gamma_{0,1}} \tag{11}$$

The reflected voltage $V_r(t)$ in literature [13] was decomposed into 'wavefront' and 'nonwavefront' components and the reflection coefficient $\Gamma_{i-1,i}$ between Z_{i-1} and Z_i such that $i \geq 2$ was expressed as follows [13].

$$
\begin{aligned}
\Gamma_{i-1,i} &= \frac{V_r(i) - V_{ref}(nonwavefront, i)}{\prod\limits_{j=1}^{j=i-1} T_{j-1,j} \prod\limits_{j=1}^{j=i-1} T_{j,j-1}} \\
&= \frac{V_r(i) - V_{ref}(nonwavefront, i)}{\prod\limits_{j=1}^{j=i-1} (1 - \Gamma_{j-1,j}^2)}
\end{aligned}
\tag{12}
$$

Therefore, the characteristic impedance Z_i of the ith uniform segment can be calculated according to Z_{i-1} and $\Gamma_{i-1,i}$, as shown in (13).

$$Z_i = Z_{i-1} \frac{1 + \Gamma_{i-1,i}}{1 - \Gamma_{i-1,i}} \tag{13}$$

The term $V_{ref}(nonwavefront, i)$ in (12) is the reflected voltage that experiences multiple reflection processes at the discontinuities formed by $Z_0, Z_1, \ldots, Z_{i-1}$ at the time of $i\Delta t$. If $Z_0, Z_1, \ldots, Z_{i-1}$ are known, $V_{ref}(nonwavefront, i)$ can be calculated by $(7) \sim (9)$ recursively.

The impedances $Z_2, Z_3, \ldots, Z_n$ then can be figured out according to $(11) \sim (13)$ iteratively with the help of the recursive multiple reflection algorithm proposed in Section 2.1.

3. EXPERIMENTS AND RESULTS

3.1. Circuits Design

To certify the multiple reflection computation method, two nonuniform microstrip lines are designed. The size of the circuit boards and the signal lines are shown in Figures 2 and 3, respectively. The impedance of the microstrip line in Figure 2 is step change and that of the microstrip line in Figure 3 is gradual change. To make sure those lines can be connected to the coaxial ports of the vector network analyzer, two location holes are designed at each side of the circuit boards. Two launchers are used in order to connect the circuits under test to vector network analyzer. The substrate of the both nonuniform lines is RO4350B, of which the relative dielectric constant and loss tangent are 3.48 and 0.004 respectively. The thickness of the substrate is 30 mil and that of the strips is 0.7 mil. The characteristic impedances of the uniform transmission line sections are computed according to [22] and shown in Table 1.
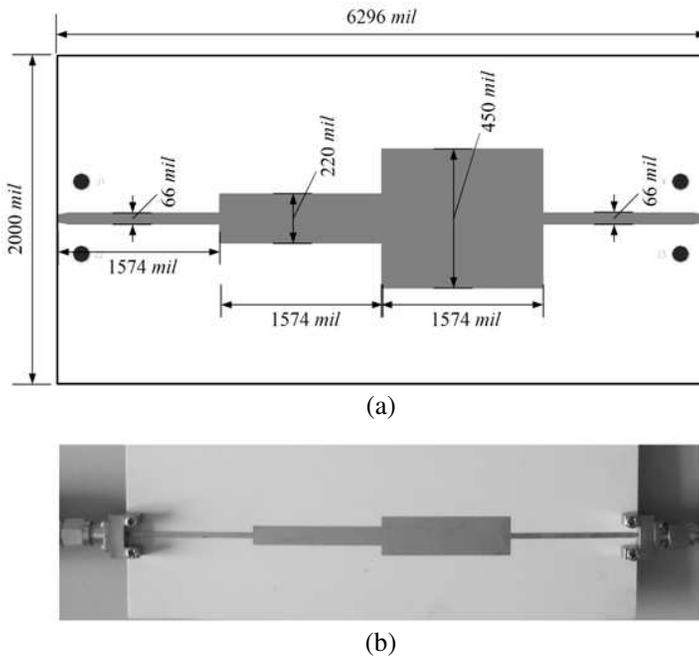

(a)

(b)

Figure 2. Nonuniform microstrip transmission line with coaxial-to-microstrip launchers. The impedance is step change. (a) Widths and lengths of the strip line sections. (b) The designed circuit board with launchers.
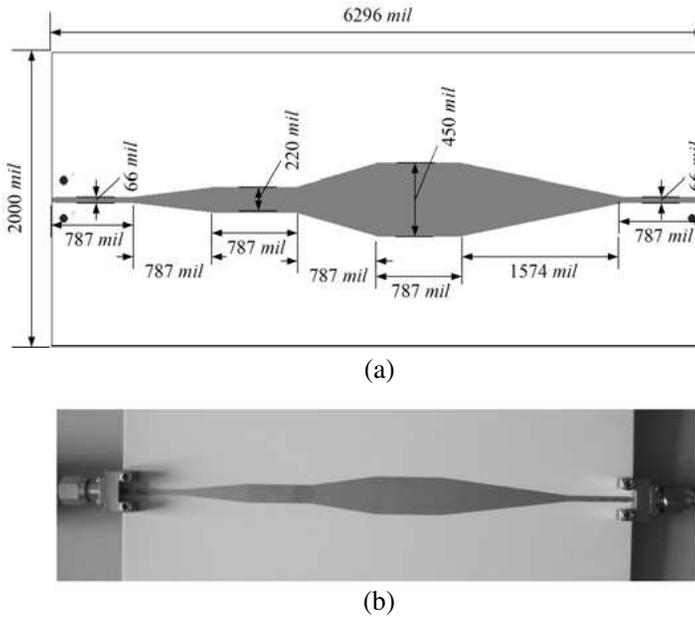
(a)

(b)

Figure 3. Nonuniform microstrip transmission line with coaxial-to-microstrip launchers. The impedance is gradual change. (a) Widths and lengths of the strip line sections. (b) The designed circuit board with launchers.

Table 1. Characteristic impedances of uniform microstrip line sections with different widths. The thickness of the strips is 0.7 mil.

Strip Width (mil)	66	220	450
Impedance (Ω)	50.6	21.3	11.6

3.2. Reconstruction Results

The microstrip lines in Figures 2 and 3 are measured from 10 MHz to 20 GHz with 10 MHz interval via Agilent vector network analyzer PNA E8363B. Usually the unit step responses of the circuits are obtained using inverse Fast Fourier Transform (IFFT). To improve the resolution of the responses of the microstrip lines in time domain, inverse Chirp-Z transform (ICZT) is used actually instead of IFFT [23]. Since the Chirp-Z transform (CZT) has been realized in MATLAB as function *czt*, the ICZT transform of scattering parameters of the microstrip lines can be determined according to the relationship between CZT

and ICZT [24], just as (14).

$$\text{ICZT}[X(k)] = (\text{CZT}[X^*(k)])^* \tag{14}$$

where the "$*$" means complex conjugate.

The unit step responses of the microstrip lines in Figures 2 and 3 can be obtained according to (15).

$$R(k) = \text{ICZT}\left[\frac{S_{11}(k)}{1 - e^{-jk(2\pi/(N+1))}}\right] \tag{15}$$

where $k = 0, 1, 2, \ldots, N$, and N is the number of S_{11}. The value of

$$\frac{S_{11}(k)}{1 - e^{-jk(2\pi/(N+1))}}$$

at $k = 0$ is obtained by extrapolating.

The hanning window [25] is used to smooth the results when employing ICZT to compute the unit step response. The unit step responses are actually corresponding to the reflection coefficients of the microstrip lines measured by TDR. Therefore the impedances of the microstrip lines can be derived according to TDR principle shown in (16).

$$Z = Z_0 \cdot \frac{1 + \rho}{1 - \rho} \tag{16}$$

where ρ is the reflection coefficient of the device under test in time domain and Z_0 is the characteristic impedance of the test port of TDR.

The reflection coefficients of the two nonuniform lines in Figures 2 and 3 are shown in Figure 4. To ensure the resolution in time domain, the time interval is set 1.25 ps and the data number is 2000. If the incident voltage V which is shown in (3a), is assumed to be 1 V, the reflection coefficient is the same as the reflected voltage V_r attained by TDR. The impedances of the nonuniform microstrip lines are computed from the corresponding reflection coefficients according to (16) and the results are shown in Figure 5. Comparing with the data in Table 1, the impedance profiles of the microstrip lines in Figure 5 don't reflect the true profiles of the nonuniform transmission lines. The multiple-reflection effect is included in the data shown in Figures 4 and 5.

To get the true impedance profiles, both the reconstruction method in this paper and Izydorczyk's algorithm are implemented to the reflection coefficients in Figure 4 and the reconstructed impedance profiles of the nonuniform microstrip lines are shown in Figures 6 and 7. The black dashed lines represent the reconstructed characteristic impedance profiles using the method in this paper; the green dash-dotted lines represent the reconstructed results using the Izydorczyk's algorithm; and the blue dotted lines represent the impedance profiles computed according to TDR principle.

The reconstructed impedance profiles agree with those computed according to the TDR principle in the first part of the traces. This is because the multiple reflection does not affect the impedance profiles of the first part. From the reconstructed characteristic impedance profiles of the microstrip lines in Figures 6 and 7, the ripples at 0.19 ns and 2.19 ns in Figure 6 and those at 0.19 ns and 2.14 ns in Figure 7 are due to mismatch of the coaxial-to-microstrip launches that are shown in Figures 2 and 3.
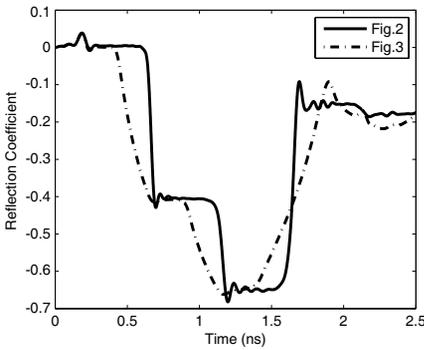

Figure 4. Reflection coefficients of the microstrip lines in Figures 2 and 3.
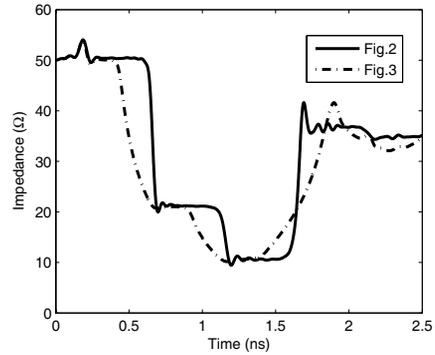

Figure 5. Impedance profiles of the nonuniform microstrip lines before reconstruction. The traces are calculated according to TDR principle.
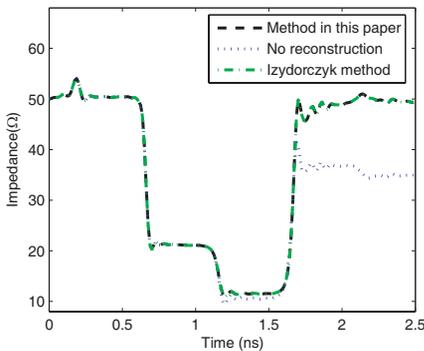

Figure 6. Comparison of the impedance profile of the microstrip line in Figure 2 before and after reconstruction.
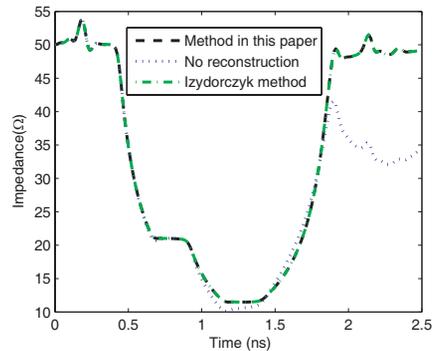

Figure 7. Comparison of the impedance profile of the microstrip line in Figure 3 before and after reconstruction.

Comparing with the impedance profiles reconstructed by the method in this paper and the Izydorczyk's algorithm, the consistency of the results validates the method in this paper.

3.3. Discussion

To make the recursive multiple reflection computation algorithm in (7) and (8) more efficient, the recursive algorithm of multiple reflection computation is realized using iterative procedure. The pseudocode of the multiple reflection computation and impedance reconstruction procedures is illustrated in Appendix A. The processing time of the algorithm is in the order of $o(N^2)$, namely if the number of uniform line segments becomes $2N$ from N, the computation time will be roughly four times longer. The Izydorczyk algorithm in literatures [20] and [21] is also in the order of $o(N^2)$. Comparing with $o(N\lfloor(N + 1)^2 - N - 1\rfloor)$ which can be expressed by $o(N^3)$ in literature [15], the multiple reflection computation algorithm in this paper and Izydorczyk's algorithm are more efficient. The time consumption of the method in this paper and Izydorczyk's algorithm for different numbers of data are compared in Table 2. The computation time in Table 2 may change slightly for different programmers. The results in Table 2 show that the method in this paper is faster than Izydorczyk's algorithm.

In Figure 6, the reconstructed impedance profile after $t = 1.7$ ns, and that in Figure 7 after $t = 1.9$ ns are not recovered totally from the raw reflection coefficients according to Table 1. To fully understand the multiple reflection computation algorithm, the characteristic impedance profiles of the nonuniform lines are reconstructed again according to the reflection coefficients in time domain measured from the both ports of each circuit board. The two impedance profiles of each microstrip lines are compared and shown in Figures 8 and 9, respectively. In Figure 8, the dash-dotted line represents the characteristic impedance which is reconstructed according to the reflection coefficients in time domain measured from prot 2 (the right port in Figure 2). The dash-dotted impedance profile

Table 2. Computation time comparison for different data points (CPU: AMD Sempron (tm) 3000+, 1.61 GHz. DDR 896 MB). The time may change for different computers and different programmers.

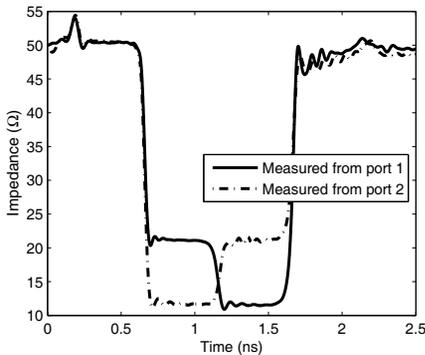| Data Number	2000	5000	10000
Method in this paper	104 ms	319 ms	993 ms
Izydorczyk algorithm	114 ms	408 ms	1990 ms

Figure 8. Impedance profiles of the microstrip line in Figure 2 after reconstruction. The traces are figured out according to coefficients from the two ports of the circuit respectively.

Figure 9. Impedance profiles of the microstrip line in Figure 3 after reconstruction. The traces are figured out according to coefficients from the two ports of the circuit respectively.
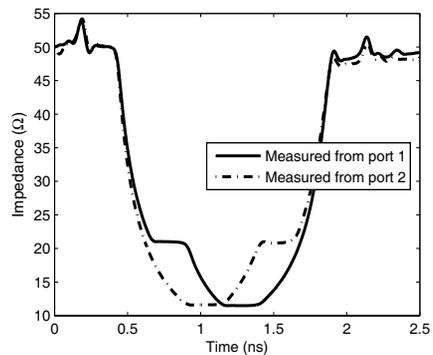
after $t = 1.7$ ns is also not recovered totally. This situation also happens in Figure 9.

In this paper, the relationship of transmission coefficient T and the reflection coefficient Γ between adjacent uniform sections is defined as

$$T = 1 + \Gamma \qquad (17)$$

In (17) the loss of the nonuniform transmission lines is not considered. This relationship is also used in [13] and [15]. However, the circuits in the experiments are not entirely lossless. The loss tangent of the substrate RO4350B is 0.004. The dielectric loss makes the differences between the reconstructed results and computed results in Table 1. Besides, the conductor loss and radiation loss [26] of the circuits also affect the process of true impedance profile reconstruction. Therefore, as well as [13] and [15], the recursive algorithm for multiple reflection computation is only suitable for lossless and low lossy nonuniform transmission lines.

4. CONCLUSION

In this paper, an explicit and effective recursive method for multiple reflection computation is present. This recursive algorithm is realized using iterative procedure and the processing time of this algorithm is in the order of $o(N^2)$. In TDR measurements, to improved the resolution

in time domain, more data are need. This algorithm is especially useful in this situation.

ACKNOWLEDGMENT

APPENDIX A. PSEUDOCODE OF MULTIPLE REFLECTION COMPUTATION AND IMPEDANCE RECONSTRUCTION

The recursive algorithm of multiple reflection computation and impedance reconstruction can be represented as the following piece of pseudocode. This algorithm is realized by the way of iteration.

for all $i = 0$ to $Datanum$ **do**
   $Lattice[i].l \leftarrow 0$
   $Lattice[i].r \leftarrow 0$
   $Gamma[i] \leftarrow 0$
   $ZLine[i] \leftarrow 0$
end for
$Gproduct \leftarrow 1$
$Z0 \leftarrow 50$
$vr\_temp \leftarrow 0$
if $Datanum \geq 1$ **then**
   $Gamma[1] \leftarrow Vtdr[1]$ {Voltage measured by TDR}
   $Lattice[1].l \leftarrow$ STEPVOLTAGE {STEPVOLTAGE=1}
   $Gproduct \leftarrow Gproduct * (1 - Gamma[1] * Gamma[1])$
else
   return
end if
if $Datanum \geq 2$ **then**
   $vr\_temp \leftarrow (1 - Gamma[1]) * Lattice[1].r + Gamma[1] * Lattice[1].l$
   $Gamma[2] \leftarrow (Vtdr[2] - vr\_temp)/Gproduct$
   $Lattice[2].l \leftarrow Lattice[1].l * (1 + Gamma[1])$
   $Lattice[1].r \leftarrow Lattice[2].l * Gamma[2]$
   $Gproduct \leftarrow Gproduct * (1 - Gamma[2] * Gamma[2])$
else
   return
end if

for $i = 3$ to $Datanum$ **do**
    $Lattice[i].l \leftarrow Lattice[i-1].l * (1 + Gamma[i-1])$
    $Lattice[i-1].l \leftarrow Lattice[i-2].l*(1+Gamma[i-2])+Lattice[i-2].r*(-Gamma[i-2])$
    for $k = i - 2$ to 2 **do**
        $Lattice[k].r \leftarrow Gamma[k+1]*Lattice[k+1].l+(1-Gamma[k+1])*Lattice[k+1].r$
        $Lattice[k].l \leftarrow (1 + Gamma[k-1]) * Lattice[k-1].l + (-Gamma[k-1]) * Lattice[k-1].r$
    end for
    $Lattice[1].r \leftarrow Lattice[2].l * Gamma[2] + Lattice[2].r * (1 - Gamma[2])$
    $vr\_temp \leftarrow (1-Gamma[1])*Lattice[1].r+Gamma[1]*Lattice[1].l$
    $Gamma[i] \leftarrow (Vtdr[i] - vr\_temp)/Gproduct$
    $Gproduct \leftarrow Gproduct * (1 - Gamma[i] * Gamma[i])$
    $Dincrese \leftarrow Lattice[i].l * Gamma[i]$
    $Lattice[i-1].r \leftarrow Lattice[i-1].r + Dincrese$
    for $k = i - 2$ to 1 **do**
        $Dincrese \leftarrow Dincrese * (1 - Gamma[k + 1])$
        $Lattice[k].r \leftarrow Lattice[k].r + Dincrese$
    end for
end for
$ZLine[0] \leftarrow Z0$
for $i = 1$ to $Datanum$ **do**
    $ZLine[i] \leftarrow (1 + Gamma[i])/(1 - Gamma[i]) * ZLine[i - 1]$
end for

REFERENCES

1. Lin, D.-B., I.-T. Tang, and Y.-Y. Chang, "Flower-like CPW-FED monopole antenna for quad-band operation of mobile handsets," *Journal of Electromagnetic Waves and Applications*, Vol. 23, Nos. 17–18, 2271–2278, 2009.

2. Wang, W., C. Liu, L. Yan, and K. Huang, "A novel power divider based on dual-composite right/left handed transmission line," *Journal of Electromagnetic Waves and Applications*, Vol. 23, Nos. 8–9, 1173–1180, 2009.

3. Fallahzadeh, S. and M. Tayarani, "A new microstrip UWB bandpass filter using defected microstrip structures," *Journal of Electromagnetic Waves and Applications*, Vol. 24, No. 7, 893–902, 2010.

4. Zhang, G.-H., M. Xia, and X.-M. Jiang, "Transient analysis of wire structures using time domain integral equation method with

exact matrix elements," *Progress In Electromagnetics Research*, Vol. 92, 281–298, 2009.

5. Sharma, R. Y., T. Chakravarty, and A. B. Bhattacharyya, "Transient analysis of microstrip-like interconnections guarded by ground tracks," *Progress In Electromagnetics Research*, Vol. 82, 189–202, 2008.

6. Khalaj-Amirhosseini, M., "Analysis of nonuniform transmission lines using the equivalent sources," *Progress In Electromagnetics Research*, Vol. 71, 95–107, 2007.

7. Sheen, D. and D. Shepelsky, "Uniqueness in the simultaneous reconstruction of multiparameters of a transmission line," *Progress In Electromagnetics Research*, Vol. 21, 153–172, 1999.

8. Navarro, L., E. Mayevskiy, and T. Chairet, "Application of launch point extrapolation technique to measure characteristic impedance of high frequency cables with TDR," *Design Conference*, 2009.

9. Chen, S.-D. and C.-K. C. Tzuang, "Characteristic impedance and propagation of the first higher order microstrip mode in frequency and time domain," *IEEE Transactions on Microwave Theory and Techniques*, Vol. 50, No. 5, 1370–1379, May 2002.

10. Xie, H., J. Wang, D. Sun, R. Fan, and Y. Liu, "Spice simulation and experimental study of transmission lines with TVSs excited by EMP," *Journal of Electromagnetic Waves and Applications*, Vol. 24, Nos. 2–3, 401–411, 2010.

11. Ostwald, O., "Time domain measurement using vector network analyzer ZVR," *ZVR Application Note*, May 1998.

12. Agilent Technologies, "Time domain analysis using a network analyzer," *Application Note*, 1287-12, 2007.

13. Hsue, C.-W. and T.-W. Pan, "Reconstruction of nonuniform transmission lines from time-domain reflectometry," *IEEE Transactions on Microwave Theory and Techniques*, Vol. 45, No. 1, 32–38, January 1997.

14. TDA Systems, "PCB interconnect characterization from TDR measurements," *Application Note*, 1999.

15. De Pádua Moreira, R. and L. R. A. X. de Menezes, "Direct synthesis of microwave filters using inverse scattering transmission-line matrix method," *IEEE Transactions on Microwave Theory and Techniques*, Vol. 48, No. 12, 2271–2276, 2000.

16. Jong, J. M., V. K. Tripathi, L. A. Hayden, and B. Janko, "Lossy interconnect modeling from TDR/T measurements," *IEEE 3rd Topical Meeting on Electrical Performance of Electronic*

Packaging, 133–135, 1994.

17. Jaggard, D. L. and P. V. Frangos, "The electromagnetic inverse scattering problem for layered dispersionless dielectrics," *IEEE Transactions on Antennas and Propagation*, Vol. 35, No. 8, 934–946, 1987.

18. Lin, C. J., C. C. Chiu, S. G. Hsu, and H. C. Liu, "A novel model extraction algorithm for reconstruction of coupled transmission lines in high-speed digital system," *Journal of Electromagnetic Waves and Applications*, Vol. 19, No. 12, 1595–1609, 2005.

19. Gu, Q. and J. A. Kong, "Transient analysis of single and coupled lines with capacitively-loaded junctions," *IEEE Transactions on Microwave Theory and Techniques*, Vol. 34, No. 9, 952–964, 1986.

20. Izydorczyk, J., "Comments on "Time-domain reflectometry using arbitrary incident waveforms"," *IEEE Transactions on Microwave Theory and Techniques*, Vol. 51, No. 4, 1296–1298, 2003.

21. Izydorczyk, J., "Microwave time domain reflectometry," *Electronics Letters*, Vol. 41, No. 15, 848–849, 2005.

22. Pozer, D. M., *Microwave Engineering*, 3rd edition, John Wiley & Sons, Inc, 2005.

23. Yiding, W., W. Yirong, and H. Jun, "Application of inverse Chirp-Z transform in wideband radar," *IEEE 2001 International Geoscience And Remote Sensing Symposium*, Vol. 4, 1617–1619, 2001.

24. Frickey, A., "Using the inverse Chirp-Z transform for time-domain analysis of simulated radar signals," *Proceedings of the 5th International Conference on Signal Processing Applications and Technology*, 1366–1371, 1995.

25. Harris, F. J., "On the use of windows for harmonic analysis with the discrete fourier transform," *Proceedings of the IEEE*, Vol. 66, No. 1, 51–83, 1978.

26. Faraji-Dana, R. and R. L. Chow, "The current distribution and ac resistance of a microstrip structure," *IEEE Transactions on Microwave Theory and Techniques*, Vol. 38, No. 9, 1268–1277, 1990.